CIÊNCIA EXATAS E DA TERRA

Scientia Amazonia, v. 11, n.2, C1-C11, 2022
Revista on-line http://www.scientia-amazonia.org
https://doi.org/10.5281/zenodo.7063085 ISSN:2238.1910

DFT method in ALA, DHA and EPA molecules in Raman vibrational analysis of ostrich oil from the Amazon

Asaf Ribas[1*], Roberta Cristina Lima[1], Quesle da Silva Martins[1]

Abstract

Density Functional Theory (DFT) method was applied in the process of vibrational investigation in fatty acid structures: eicosapentaenoic (EPA), docosahexaenoic (DHA), alpha-linolenic or linolenic (ALA). The data were crossed with response of Raman spectroscopy in ostrich oil (OA). In this study, the Raman spectrum of pure ostrich oil presents a vibrational pattern common to many oils, even from different origins, and the association with DFT calculations was important to define the vibrational signature of chemical bonds, mainly from groups C=O, C=C, CH_2 present in ALA, DHA and EPA.

Keywords: DFT method, Raman Spectroscopy, Ostrich oil.

Resumo

O método da Teoria Funcional da Densidade (DFT) foi aplicado no processo de investigação vibracional em estruturas de ácidos graxos: eicosapentaenóico (EPA), docosahexaenóico (DHA), alfa-linolênico ou linolênico (ALA). Os dados foram cruzados com resposta da espectroscopia Raman em óleo de avestruz (OA). Neste estudo, o espectro Raman do óleo de avestruz puro apresenta um padrão vibracional comum a muitos óleos, mesmo de origens diferentes, e a associação com cálculos de DFT foi importante para definir a assinatura vibracional das ligações químicas, principalmente dos grupos C=O, C =C, CH2 presente em ALA, DHA e EPA.

Palavras-chave: Método DFT, Espectroscopia Raman, Óleo de avestruz.

[1] Fundação Universidade Federal de Rondônia - UNIR Correspondence: asafribas@hotmail.com

Scientia Amazonia, v. 11, n.2, C1-C11, 2022
Revista on-line http://www.scientia-amazonia.org
https://doi.org/10.5281/zenodo.7063085 ISSN:2238.1910
CIÊNCIA EXATAS E DA TERRA

1. Introduction

The fatty acids - AF eicosapentaenoic (EPA), docosahexaenoic (DHA) and alpha-linolenic or linolenic (ALA) are polyunsaturated fatty acids (PUFA) of the omega-3 type. The first of these is present in the composition of various vegetable oils. Whereas EPA and DHA are widely associated with oils from marine sources, such as fish and crustaceans (MARTIN 2006; MAKI 2009; ULSEN 2011). Papers corroborate that the importance of essential AF, such as omega-3, is associated with its therapeutic characteristics, anti-inflammatory, antibacterial and anti-fungal activities (ALI 2016; BAETEN 1996; HORBANCZUK 2004; SMITH 2011; DONG 2013; GAVANJI 2013). Because of these characteristics, many oils have been marketed, associating them with these components and their pharmaceutical effects. Rich in omega-3, OA contains a large concentration of AF, which includes ALA (MARTINS 2019). In general, ALA is consumed through food, whose benefits are possible due to the conversion into EPA and DHA by the organism, which can be obtained through the regular consumption of fish or supplementation (SWANSON 2012; KILLEN 2019), thus being considered essential oils (ZHOU 2013). However, studies indicate that only a small amount can be synthesized in the body in this way (NEFF 2011). An alternative source may be OA, because it has its value associated with its high composition in AF and is therefore widely traded often indiscriminately. Ostrich oil, in addition to containing ALA, contains linoleic acid and high oleic acid content (KRAWCZYK 1997; BAUNY 2007), vitamins and amino acids (FARAHPOUR 2016). Studies indicate that OA has rapid absorption by human skin, unlike petroleum products (BASUNY 2011). They also point to the control of hypertension, risk of stroke, decreased effects of arthritis and increased survival rates of autoimmune diseases (PALANISAMY 2011). It has also been studied in the manufacture of bioactive encapsulated emulsions to increase the stability of commercial products (PONPHAIBOON 2018).

In this study, the OA sample was analyzed by Raman Spectroscopy (RS) spectroscopy, which obtains sample information from the incidence of a light. In short, RS provides information on molecular linkages in the form of energy bands (vibrational modes) that are a kind of digital print of the sample. The choice for the technique is justified because it is non-invasive, fast data acquisition, with high precision in the results and widely used in the process of materials characterization (BAETEN 2010; BEER 2011; ABKARI 2016; SILVA 2018; MARTINS 2020). Computational chemistry calculations were performed for ALA, EPA and DHA molecular structures. Theoretical spectra were obtained from the calculations that were compared with the OA Raman spectrum. In addition to the theoretical spectra, the calculations provided the vibrational modes of the atomic bonds of the studied molecules. In computational calculations, the Density Functional Theory (DFT) method with B3LYP/6-31G(d,p) parameters was used (LAM 2020; JAYARAJ 2020; KUZMIN 2020). The Energy Parameter Maximum (EPM) of each molecule, obtained in VEDA, was used to identify the potential energy distribution (PED) of each vibrational mode.

The present study focused on the study of OA vibrational properties by RS, as well as on the attributions of ALA, EPA and DHA vibrational modes by DFT method, since there are few studies that apply this methodology to OA. RS was an important process of OA characterization and computational calculations helped identify bands and vibrational modes of this material. The data collected can help understand the composition of the material through the presence of PUFA among other superior AF, as well as to support the basic and advanced research of regional development of the Amazon.

2. Material and Method

2.1 Ostrich Oil

OA was extracted from the regional fauna of the State of Rondônia - Brazil. Obtained from the fat removed from glands in the abdominal region of the animal. The pure sample was transferred by local producers as the final marketing product, stored in opaque containers and at room temperature.

Scientia Amazonia, v. 11, n.2, C1-C11, 2022
Revista on-line http://www.scientia-amazonia.org
https://doi.org/10.5281/zenodo.7063085 ISSN:2238.1910

2.2 Raman Spectroscopy

Raman spectra were obtained using confocal laser scanning microscopy (CLSM), in a Horiba Xplora Raman series with spectral range from 0 to 4000 cm^{-1}, single *laser* 532 nm, confocal image 0.5 um (XY) in high resolution. The experimental spectra are in the region from 500 to 1850 cm^{-1}, for comprising a region of interest (digital print region of the sample). The experimental measurements were performed at the Laboratory of Characterization and Microscopy of Materials (LCMMAT) of Universidade Federal de Alagoas (UFAL).

2.3 DFT method

The DFT method was used in the GAUSSIAN 09 computational package (FRISCH *et al*. 2009), providing frequencies and vibrational modes of ALA, DHA and EPA molecules. In the DFT calculation, the hybrid function (BECKE 1993; HUANG 2016) of three parameters (B3) was utilized, used for a non-local change of functional terms (LYP). The LYP correlation function is accepted as the most cost-effective approach to calculate the molecular structure, vibrational frequencies, and energy of optimized structures (LEE 1988; WU 2012). In addition to the functional (B3LYP), the polarized base set 6-31G(d,p) was employed in the process. Polarization ("d" and "p") indicates a more accurate performance over hydrogen and oxygen atoms, respectively. Vibrational attributions and potential power distribution (PED) were made with a high degree of precision by the VEDA software (JAMROZ 2013).

3. Results and Discussion

Figure 1 shows the Raman spectra of the suspended oil sample with 532 nm green *laser* excitation. Vibrational bands appear in 1079, 1113, 1263, 1300,1440, 1655, 1743 cm^{-1}. These bands are very common in samples containing various fatty acids (MARINA 2009; VARGAS 2014; LIMA 2015; RUI 2019; WERONIKA 2020). The most intense bands are marked at 1440 and 1655 cm^{-1}. The band at 1440 cm^{-1} can be attributed to CH_2 deformation mode and the band at 1655 cm^{-1} is attributed to unsaturated fatty acid C=C bond groups, as well as bands in 1300, 1263 and 1079 cm^{-1} (HUANG 2016; LI 2018). Considering the presence of structures containing carbonyl group and the presence of unsaturated groups, the presence of the band at 1655 cm^{-1} corresponds precisely to a typical symmetrical stretching pattern of C=C. A band in 1155 cm^{-1} has a characteristic of the symmetrical stretching mode C–C of carotenoids, as well as the band in 1525 cm^{-1}, attributed to the symmetrical stretching mode of the C=C bond of carotenoids (JIN 2019; WITHNALL 2012; MACERNIS 2014). It is possible to see this band in the oil spectrum of Buriti associated with the presence of the ester function (ALBUQUERQUE 2003). The absence of these modes in the OA spectrum may be a decisive factor when comparing samples from different sources, since these modes are not present in the sample under study. In Figure 1, the band at 1743 cm^{-1} is attributed to the symmetrical stretching vibration of C=O of the carboxylic groups, as observed in a study of Brazilian Nut oil (MARTINS 2020). In general, the bands shown in Figure 1 are more intense for bonds of symmetric groups and less intense for asymmetric bonds. It also brings wide bands as they decrease in wave number, as seen for the band at 865 cm^{-1}, due to the large number of CH groups contained in this type of sample. In Figure 2, the frequencies calculated at 1745 cm^{-1} for DHA, at 1733 and 1745 cm^{-1} for EPA and 1703 and 1720 cm^{-1} in ALA have good correspondence with the OA bands. For example, the band at 1743 cm^{-1}can be assigned to the ester-carbonyl bond, as well as the stretching mode in the region of 1745 cm^{-1} (HUANG 2016; AYKAS 2020; SENESI 2021).

Scientia Amazonia, v. 11, n.2, C1-C11, 2022
Revista on-line http://www.scientia-amazonia.org
https://doi.org/10.5281/zenodo.7063085 ISSN:2238.1910
CIÊNCIA EXATAS E DA TERRA

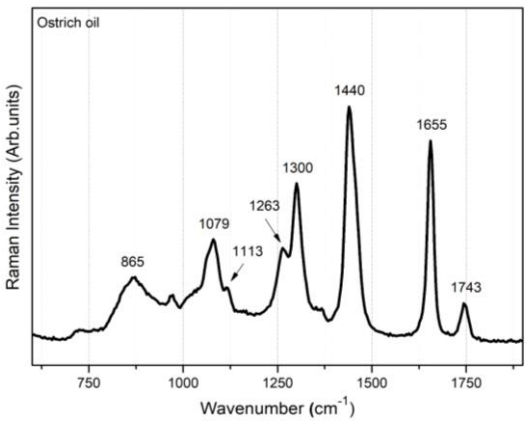

Figure 1: Experimental Raman spectrum of pure OA. The region between 500 - 1850 cm^{-1} comprises the digital print region of the spectrum.

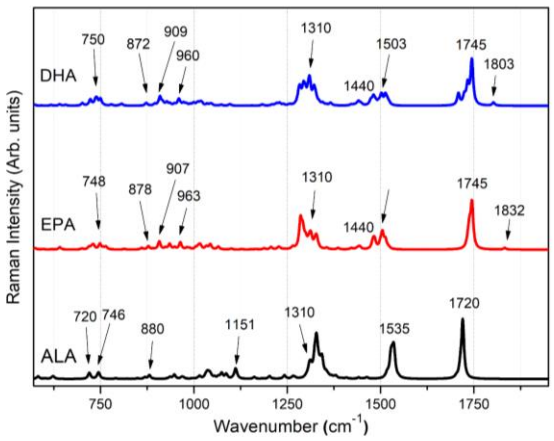

Figure 2: Raman Spectra calculated from DHA (blue), EPA (red) and ALA (black) molecules. The region between 500 - 1850 cm^{-1} comprises the digital print region of the spectrum.

Figure 3 shows theoretical spectra, result of computational calculation, based on the DFT method for DHA (blue), EPA (red) and ALA (black) molecules. The results are based on molecular optimization for the molecules fundamental state. The spectra in Figure 2 are in the region between 500 and 1850 cm^{-1}. These spectra present distinct regions of Raman activities: one below 1250 cm^{-1}, one between 1250 and 1350 cm^{-1}, between 1440 and 1550 cm^{-1} , and between 1700 and 1850 cm^{-1} . The region below 1250 cm^{-1} has stretching and torsion modes of the structures. Between 1250 and 1350 cm^{-1}, deformation modes predominate and 1440 cm^{-1}, stretch and deformation modes are present. The EPM value was considered in the data calculated to identify the respective vibrational modes that can be seen in Table 1. Table 1 also brings the values of molecular polarizability (α) in arbitrary units (a.u.) and the conformation energies (in Hartree) to each molecule. The highest conformation values (in module) after convergence are for DHA. Among the structures, the one that presented the greatest convergence efficiency (EPM) was ALA. In Figure 2, DHA and EPA present vibrational bands at 1745 cm^{-1}, as well as a band at 1440 cm^{-1}, respectively. At first, these (theoretical) bands may be related to experimental data. In fact, the results of the calculation showed that the band 1440 cm^{-1} is associated with the C-C symmetrical stretch mode of the structures, however, the band 1745 cm^{-1}associated with the symmetric C=stretch mode shown in Figure 1, does not correspond to this cluster, but to the C=C stretch mode in DHA and EPA. This can be explained because EPA and DHA structures have a greater number of unsaturations, 5 and 6 respectively, which make the molecular bond more rigid, increasing the frequency of vibration. The C=O bond is responsible for the low intensity band that appears at 1832 cm^{-1} for EPA and 1803 cm^{-1} for DHA. The low bands intensity is related to the selection factor of vibrational modes in Raman spectroscopy, where for non-symmetric groups, there is low energy absorption, reflecting directly on the intensity of these, which is in accordance with the calculated data (LARKIN 2011). Another relevant factor in Figure 2 is the position of the C=O band for DHA and EPA, which are in a region well above that observed in Figure 1, and which may have another explanation, which may be related to the electronegativity of the atoms involved. Because it is more electronegative than other bonds in the molecule, the C=O

Scientia Amazonia, v. 11, n.2, C1-C11, 2022
Revista on-line http://www.scientia-amazonia.org
https://doi.org/10.5281/zenodo.7063085 ISSN:2238.1910
CIÊNCIA EXATAS E DA TERRA

bond steals more electrons from the set, becoming stronger, which ends up interfering in the band's position as to the frequency of vibration (ARROIO 2010). Figure 3 shows the maps of electrostatic potential (MEP) of ALA, EPA and DHA molecules, showing that the region of C=O bond is more electronegative (in red). In the ALA spectrum, the band centered at 1720 cm^{-1} is designated by the symmetrical stretch of C=C bond and is combined with C=O stretch mode at 1721 cm^{-1}. It is noted that this band exists in a region that would be between two important bands for oils containing fatty acids. In spectrum calculated of ALA, the band at 1440 cm^{-1} appears from spectra calculated at 1310 cm^{-1} combined with other bands. This band may be associated with the folding of the HCC molecular group and of CH_2 groups or conjugates of the C=C bonds unsaturations (MARTINS 2019; JIN 2019) and may refer to the existing band in 1300 cm^{-1} of the experimental spectrum. Torsion modes of HCCC clusters are obtained in 746 cm^{-1} (ALA), 748 cm^{-1} (DHA) and 750 cm^{-1} (EPA).

Table 1: General information about the calculated Gaussian 09 parameters and VEDA software data.

Molecule	Energia (Hartree)	EPM (%)	Polarization (Debye)	Polarizability (a.u.)
ALA (18:3)	-854.374	53.07	1.655	210.795
DHA (22:6)	-1008.005	51.28	1.018	240.762
EPA (20:5)	-930.606	48.29	1.130	218.643

Table 2 shows the calculated frequencies (ω_{calc}) accompanied by vibrational signatures. It also brings the experimental frequencies (ω_{exp}) of the bands marked in Figure 1. To the ω_{calc} frequencies the percentage factor of vibrational contribution is assigned, considering only values above 10%. Observing Table 2 $\omega_{, calc}$ frequencies for C=O bonds, present a higher vibrational contribution factor with values above 79%. The vibrational contribution is lower for the frequencies 1111 cm^{-1} (ALA), 963 cm^{-1} (EPA) and 960 cm^{-1} (DHA), all associated with CC bond stretching modes. The frequencies calculated in the region below 1250 cm^{-1} bring low intensity bands (see Figure 2). These bands present modes of stretches (ν) and folds (δ) assigned to more than one cluster of atoms. Torsion modes (τ) are verified in 720 and 746 cm^{-1} of ALA molecule, 907 and 748 cm^{-1} for EPA and 750 cm^{-1} for DHA molecule. As they are long chain structures, we have that frequencies 720, 748 and 750 cm^{-1} are also related to stretching and deformation modes of CH_2. Another relevant fact is the conformation of the molecules shown in Table 2. In PUFA, long-chain molecules, the profile of molecular conformation can be a direct response of unsaturated molecules in the molecule (HARVEY 2011), presenting less deformation than with a smaller set of unsaturated fats, on the other hand, the higher number of unsaturated agents, the more expected deformations, that is, torsions along the chain. This is due to *the cis* double bond that forces a fold in the hydrocarbon chain (YANG 2011, AHMAD 2017). This behavior can be seen in the figures in Table 2 (and in Figure 3) for ALA, EPA and DHA molecules. The ALA molecule that contains three unsaturations in the primary chain has conformation with less deformation. EPA contains five unsaturations and DHA contains six, indicating a larger set of torsions, which is in accordance with Yang (2011) and Ahmad (2017). In addition to torsion modes, Table 2 shows stretching and deformation modes for C=C bonds or that contain the same. On the types and classification of vibrational modes, this study presents stretching modes: symmetric (ν_s) and asymmetric (ν_{as}) and, angular deformations: rocking (δ_r), scissoring (δ_{sci}). The molecules shown in

Scientia Amazonia, v. 11, n.2, C1-C11, 2022
Revista on-line http://www.scientia-amazonia.org
https://doi.org/10.5281/zenodo.7063085 ISSN:2238.1910
CIÊNCIA EXATAS E DA TERRA

Table 2 were generated in the Gauss View program from .chk extension files. The colors indicate: dark gray for carbon atoms, light gray for hydrogen and red, oxygen.

Table 2: ALA, EPA, DHA vibrational signatures in Gaussian 09. Contributions of vibrational modes are from VEDA.

ω_{exp}	ω_{calc}	Assignments	Estructures
		ALA	
1743	1721	ν(C=O) (23 22) [79]	
	1720	ν(C=C) (26 28) [67]	
		ν(C=C) (33 35)	
		ν(C=C) (40 42)	
1655		ν(C=C) (26 28)	
1440	1441	δ(HCH) (48 47 49) [81]	
	1328	δ(HCC) (29 28 30) [54]	
1300	1310	δ(HCC) (21 19 26) [14]	
1263	1262	δ(HCC) (38 37 40) [27]	
1113	1111	ν(CC) (7 10) [22]	
1079			
	881	ν(CC) (44 42) [45]	
	746	τ(HCCC) (43 42 40 37) [54]	
	720	τ(HCCC) (27 28 26 30) [56]	
ω_{exp}	ω_{calc}	Assignments	Estructures
		EPA	
	1832	ν_s(C=O) (2 11) [85]	
1743	1745	ν(C=C) (9 12) [66]	
	1738	ν(C=C) (19 21) [71]	
	1733	ν(C=C) (17 18) [58]	
		ν(C=C) (14 16)	
		ν(C=C) (6 8)	
1655			
	1504	δ(HCH) (37 13 38) [69]	
1440	1439	δ(HCC) (33 9 12) [67]	
1300	1299	τ(HCCC) (40 15 19 21 [34]	

Scientia Amazonia, v. 11, n.2, C1-C11, 2022
Revista on-line http://www.scientia-amazonia.org
https://doi.org/10.5281/zenodo.7063085 ISSN:2238.1910
CIÊNCIA EXATAS E DA TERRA

1263	1265	τ(HOC) (23 3 5 11) [22]	
	963	ν(CC) (17 13) [13]	
	907	τ(HCCC) (43 17 18 15) [16]	
	878	ν(CC) (20 21) [47]	
	748	τ(HCCC) (42 16 14 10) [49]	

ω_{exp}	ω_{calc}	Assignments	Estructures
		DHA	
	1803	ν_s(C=O) (2 23) [84]	
1743	1745	ν_s(C=C) (11 12) [70]	
	1744	ν_s(C=C) (22 20) [70]	
		ν_s(C=C) (16 17) [70]	
		ν_s(C=C) (18 19) [70]	
		ν_s(C=C) (13 15)	
		ν_s(C=C) (8 10)	
1440	1440	δ(HCC) (38 8 10) [53]	
1300	1298	δ(HCC) (45 16 17) [24]	
1079	1073	ν(CC) (14 19) [35]	
	960	ν(CC) (10 4) [12]	
	909	ν(CC) (6 16) [28]	
	872	ν(CC) (21 22) [42]	
	750	τ(HCCC) (49 20 22 21) [50]	

Legenda: ν = stretching; δ = bending; τ = torsion.

Figure 3 shows MEP, which brings the load density of the test molecules, which is the distribution of electrons responsible for the chemical behavior of each species. Regions tending to blue have higher electronegativity, in this case, associated with oxygen existence, and regions tending to red indicate lower

Scientia Amazonia, v. 11, n.2, C1-C11, 2022
Revista on-line http://www.scientia-amazonia.org
https://doi.org/10.5281/zenodo.7063085 ISSN:2238.1910

electronegativity, where hydrogens are located. MEP is the result of the method used (B3LYP), whose atomic loads are calculated according to Mulliken population analysis (MINELLY 2021).

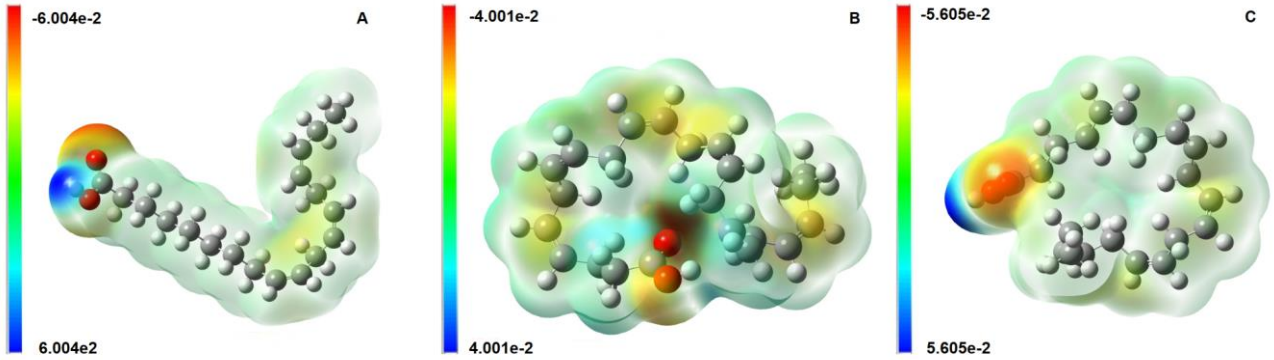

Figure 3: Electrostatic potential maps of ALA (A), DHA (B) and EPA (C) molecules. Energy spectrum with high electronic density in red color - electron-rich regions. High values of negative potential - blue scale, is spectrum of low electronic density, related to regions deficient in electrons.

4. Conclusion

Raman spectroscopy showed spectral bands of interest in the study of vibrational modes for OA. Bands centered on 1440 and 1655 and 1745 cm^{-1} were identified and associated with the presence of unsaturated groups (C=C) and carboxyl groups (C=O). In the calculated spectra, the highlight bands are mostly referred to as symmetric stretching modes of C=C and C=O group and for some deformation modes in CH_2 and CH_3 type bonds. In the identification process of vibrational modes, a displacement of bands well above the reference region (experimental) was observed for theoretical results, which was attributed to molecular unsaturation factors and correspondence with electronic affinities of molecules atoms. An easy check is the position of the calculated bands of C=O which grow in wave number in the spectra calculated for the molecule with the highest unsaturation load. Calculations of DHA and EPA molecules showed similarities in the spectral nature among themselves, especially for modes in 1310, 1440, 1503 and 1745 cm^{-1}. DFT calculations were important in the assignment of OA vibrational modes and to define the polar response and electronic characteristics of ALA, DHA and EPA molecules, and could serve as a parameter for additional studies. In addition, this study opens the possibility for a conformational analysis of the components studied or other compounds associated with OA.

Acknowledgment

The authors are grateful to the Grupo de Óptica e Nanoscopia (GON) - UFAL, Grupo de Pesquisa em Física Experimental e Aplicada - UNIR, to the laboratories Estrutura da Matéria e Física Computacional e Física Aplicada - DAF/JP/UNIR and also to the PIBIC-CNPQ (Publication number 2021/PIBIC/Dpesq/ Propesq/2021) and FAPERO (Grant number 008/2018) for financial incentives.

Disclosure

This article is unpublished and is not being considered for any other publication. The author(s) and reviewers did not report any conflict of interest during their evaluation. Thus, the journal *Scientia Amazonia* holds the copyright, has the approval and

Scientia Amazonia, v. 11, n.2, C1-C11, 2022
Revista on-line http://www.scientia-amazonia.org
https://doi.org/10.5281/zenodo.7063085 ISSN:2238.1910

permission of the authors to disclose this Article electronically.

References

Abkari A, I. Chaabane, K. Guidara, DFT (B3LYP/LanL2DZ and B3LYP/6311G+(d,p)) comparative vibrational spectroscopic analysis of organic–inorganic compound bis(4-acetylanilinium) tetrachlorocuprate(II), *Physica E*, 81, 136-144 (2016) https://doi.org/10.1016/j.physe.2016.03.010

Ahmad, M.U, Fatty acids: chemistry, synthesis, and applications. London, United Kingdom, (2017). 994643372

Ali H., Nawaz, H., Saleem, M., Nurjis, F., and Ahmed, M. Qualitative analysis of desi ghee, edible oils, and spreads using Raman spectroscopy. *J. Raman Spectrosc.*, 47, 706–711 (2016). doi: 10.1002/jrs.4891

Amany, M. M. B., Shaker, M. A., Shereen, L.N., Utilization of ostrich oil in foods, *Int. Res. J. Biochem. Bioinform,* 2(8), 199-208 (2011).

Arroio A, Honorio KM, Silva ABF, Propriedades químico quânticas empregadas em estudos das relações estrutura-atividade. *Quím Nova* 33(3), 694–699 (2010). https://doi.org/10.1590/S0100-40422010000300037

Aykas, DP; Karaman, AD; Keser, B; Rodriguez-Saona, L. Abordagem de autenticação não direcionada para azeite de oliva extra virgem. *Foods*, 9 , 221 (2020). https://doi.org/10.3390/foods9020221

Baeten V., P. Hourant, M. T. Morales, R. Aparicio, Detection of Virgin Olive Oil Adulteration by Fourier Transform Raman Spectroscopy, *Journal of Agricultural and Food Chemistry 44* (8), 2225-2230 (1996). https://doi: 10.1021/jf9600115

Baeten V., Raman spectroscopy in lipid analysis, *Lipid Tech.* 22, 36-38 (2010). https://doi.org/10.1002/lite.200900082

Balan C. Balan, IR, Raman and SERS analysis of amikacin combined with DFT-based calculations, *Spectrochim. Acta A*, (2019). https://doi.org/10.1016/j.saa.2019.02.012

Becke A.D., Density-functional thermochemistry. III. The role of exact exchange *J. Chem. Phys,* 98, 5648 (1993). https://doi.org/10.1063/1.464913

Beer T.D., *et al.*, Near infrared and Raman spectroscopy for the in-process monitoring of pharmaceutical production processes, *Int J Pharm.* bf30, 417(1-2), 32-47 (2011). https://doi.org/10.1016/j.ijpharm.2010.12.012

Dong W, Zhang Y, Zhang B, Wang X, Rapid prediction of fatty acid composition of vegetable oil by Raman spectroscopy coupled with least squares support vector machines, J *Raman Spectrosc* 44, 1739–1745 (2013). https://doi.org/10.1002/jrs.4386

Farahpour M.R., Vahid M., Oryan A., Effectiveness of topical application of ostrich oil on the healing of *Staphylococcus aureus*- and *Pseudomonas aeruginosa*-infected wounds, *Connective Tissue Research*, 59(3), 212-222 (2018). doi:10.1080/03008207.2017.1350174

Frisch M.J., *et al.,* Gaussian 09, Wallingford CT, (2009).

Gavanji S., B. Larki, A.H. Taraghian, A review of Application of Ostrich oil in Pharmacy and Diseases treatment, *Journal of Novel Applied Sciences,* 18, 650-654 (2013)

Horbanczuk, J.O., *et al.,* Cholesterol content and fatty acid composition of two fat depots from slaughter ostriches (Struthio camelus) aged 14 months, *Animal Science Papers and Reports*, *22*(2), 247-251 (2004). http://www.ighz.edu.pl/?p0=5&p1=34&l=2

Huang F, *et al.,* Identification of waste cooking oil and vegetable oil via Raman spectroscopy, *J. Raman Spectrosc*, 47, 860–864 (2016). https://doi.org/10.1002/jrs.4895

Jamróz M.H., Vibrational energy distribution analysis (VEDA): scopes and limitations, *Spectrochimica Acta Part A*, 114, 220–230 (2013). https://doi.org/10.1016/j.saa.2013.05.096

Jin Qiu, J.; Hou, H.-Y.; Yang, I.-S.; Chen, X.-B. Raman Spectroscopy Analysis of Free Fatty Acid in Olive Oil, *Appl. Sci.,* 9, 4510 (2019). https://doi.org/10.3390/app9214510

Killeen, D.P., Card, A., Gordon, K.C., Perry, N.B., First Use of Handheld Raman Spectroscopy to Analyze Omega-3 Fatty Acids in Intact Fish Oil Capsules, *Applied Spectroscopy,* 74(3), 365–371 (2020). https://doi.org/10.1177/0003702819877415

Scientia Amazonia, v. 11, n.2, C1-C11, 2022
Revista on-line http://www.scientia-amazonia.org
https://doi.org/10.5281/zenodo.7063085 ISSN:2238.1910

Lam H-Y., Roy P.K., Chattopadhyay S., Thermal degradation in edible oils by surface enhanced Raman spectroscopy calibrated with iodine values, *Vibrational Spectroscopy*, 106, 103018 (2020). https://doi.org/10.1016/j.vibspec.2019.103018

Lee C., W. Yang, R.G. Parr, Development of the Colle-Salvetti correlation-energy formula into a functional of the electron density. *Phys. Rev. B,* 98, 785 (1988). https://doi.org/10.1103/PhysRevB.37.785

Li Y., *et al.,* Detection of olive oil adulteration with waste cooking oil via Raman spectroscopy combined with iPLS and SiPLS, *Spectrochim. Acta A,* 189, 37-43 (2018). https://doi.org/10.1016/j.saa.2017.06.049

Lima T.K. Musso M, Menezes D.B, Using Raman spectroscopy and an exponential equation approach to detect adulteration of olive oil with rapeseed and corn oil, *Foody Chem.,* 333, 127454 (2020). https://doi.org/10.1016/j.foodchem.2020.127454

M.L.S. Albuquerque, I. Guedes, P. Alcantara, S.G.C. Moreira, Infrared absorption spectra of Buriti (Mauritia flexuosa L.) oil, *Vib. Spec.,* 33, 127-131 (2003). https://doi.org/10.1016/S0924-2031(03)00098-5

Macernis M, Sulskus J, Malickaja S, Resonance Raman spectra and electronic transitions in carotenoids: A density functional theory study, *J. Phys. Chem. A*, 118, 1817–1825 (2014). https://doi.org/10.1021/jp406449c

Maki KC, *et al.,* Krill oil supplementation increases plasma concentrations of eicosapentaenoic and docosahexaenoic acids in overweight and obese men and women. *Nutr Res.* 29(9), 609-15 (2009). https://doi.org/10.1016/j.nutres.2009.09.004

Marina A.M, Y. B. Che Man, S. A. H. Nazimah, I. Amin, Chemical Properties of Virgin Coconut Oil, *J. Am. Oil Chem. Soc.,* 86, 301 (2009). https://doi.org/10.1007/s11746-009-1351-1

Martin C.A, *et al.*, Ácidos graxos poliinsaturados ômega-3 e ômega-6: importância e ocorrência em alimentos. *Rev. Nutr.,* 19, 761-770 (2006). https://doi.org/10.1590/S1415-52732006000600011

Minelly M.A, *et al.,* Antileishmanial activity evaluation of a natural amide and its synthetic analogs against Leishmania (V.) braziliensis: an integrated approach in vitro and in silico, *Parasitol Res*, 120, 2199–2218 (2021). https://doi.org/10.1007/s00436-021-07169-w

Neff L.M, *et al.*, Algal Docosahexaenoic Acid Affects Plasma Lipoprotein Particle Size Distribution in Overweight and Obese Adults, *J Nutr.,* 141, 207-13, (2011). https://doi.org/10.3945/jn.110.130021

P. Jayaraj, R. Desikan, Synthesis, crystal structure, and DFT calculations of 2H-1,3-benzodioxol-5-yl 3-(4-hydroxy-3-methoxyphenyl) prop-2-enoate, *Chem. Data Collect.,* 29, 100518 (2020). https://doi.org/10.1016/j.cdc.2020.100518

P. Larkin, Infrared and Raman Spectroscopy, Principles and Spectral Interpretation, 1st Edition - Elsevier (2011).

Palanisamy U.D., et al, An Effective Ostrich Oil Bleaching Technique Using Peroxide Value as an Indicator, *Molecules,* 16(7), 5709-5719 (2011). https://doi.org/10.3390/molecules16075709

Peng H., Hou H-Y., Chen X-B., DFT Calculation and Raman Spectroscopy Studies of a-Linolenic Acid, *Quim. Nova*, 44(08), (2021). https://doi.org/10.21577/0100-4042.20170749

Ponphaiboon, Juthaporn, *et al.*,Influence of Emulsifiers on Physical Properties of Oil/Water Emulsions Containing Ostrich Oil, *Key Engineering Materials*, 777, 592–596 (2018). doi:10.4028/www.scientific.net/kem.777.592

Q.S. Martins, *et al.,* Investigation of ostrich oil via Raman and infrared spectroscopy and predictions using the DFT method, *Vib. Spec.*, 104, 102945 (2019). https://doi.org/10.1016/j.vibspec.2019.102945

Q.S. Martins, L.M.S.Santos, J.L.B.Faria, Raman spectra and ab-initio calculations in Bertholletia excelsa oil, *Vib. Spec.,* 106, 102986 (2020). https://doi.org/10.1016/j.vibspec.2019.102986

Rui H, *et al.,* Safety analysis of edible oil products via Raman spectroscopy, *Talanta*, 191, 324-332 (2019). https://doi.org/10.1016/j.talanta.2018.08.074

Senesi R, *et al.,* Looking for Minor Phenolic Compounds in Extra Virgin Olive Oils Using Neutron and Raman Spectroscopies, *Antioxidants*, 10, 643 (2021). https://doi.org/10.3390/antiox10050643

Silva C.B, *et al.,* Vibrational and structural properties of L-Alanyl-L-Phenylalanine dipeptide by Raman spectroscopy, infrared and DFT

Scientia Amazonia, v. 11, n.2, C1-C11, 2022
Revista on-line http://www.scientia-amazonia.org
https://doi.org/10.5281/zenodo.7063085 ISSN:2238.1910

calculations, *Vib. Spec.,* 98, 128–133, (2018). https://doi.org/10.1016/j.vibspec.2018.08.001

Smith G.I, *et al.,* Dietary omega-3 fatty acid supplementation increases the rate of muscle protein synthesis in older adults: a randomized controlled trial, *Am J Clin Nutr.* 93, 402-12 (2011). https://doi.org/10.3945/ajcn.110.005611

Swanson D, Swanson R, Block S.A, Mousa, Omega-3 Fatty Acids EPA and DHA: Health Benefits Throughout Life, *Adv. Nutr.,* 3, 1–7 (2012). https://doi.org/10.3945/an.111.000893

Ulven S.M, *et al.,* Metabolic effects of krill oil are essentially similar to those of fish oil but at lower dose of EPA and DHA, in healthy volunteers, *Lipids,* 46(1), 37-46 (2011). https://doi.org/10.1007/s11745-010-3490-4

V.V. Kuzmin, *et al.,* Raman spectra of polyethylene glycols: Comparative experimental and DFT study, *J. Mol. Struct., 1217, 128331* (2020). https://doi.org/10.1016/j.molstruc.2020.128331

Vargas P.V.J, Ciobotă V, Raman spectroscopy as an analytical tool for analysis of vegetable and essential oils, *Flavour Fragr. J.,* 9, 287–295 (2014). https://doi.org/10.1002/ffj.3203

Weronika R, *et al.,* FT-Raman and FT-IR studies of the gluten structure as a result of model dough supplementation with chosen oil pomaces, *J. Cereal Sci.,* 93, 102961 (2020). https://doi.org/10.1016/j.jcs.2020.102961

Withnall R, Chowdhry B.Z, Silver J, Edwards H.G.M, Oliveira L.F.C, Raman spectra of carotenoids in natural products, *Spectrochim. Acta A,* 59, 2207–2212 (2003). https://doi.org/10.1016/S1386-1425(03)00064-7

X. Wu, S. Gao, J.S. Wang, H. Wang, Y.W. Huanga, Y. Zhaod, The surface-enhanced Raman spectra of aflatoxins: spectral analysis, density functional theory calculation, detection and differentiation, *Analyst,* 137, 4226-34 (2012). http://dx.doi.org/10.1039/c2an35378d

Yang X, Sheng W, Sun GY, Lee James C-M, Effects of fatty acid unsaturation numbers on membrane fluidity and α-secretase-dependent amyloid precursor protein processing. *Neurochemistry International*, (3): 321–329, (2011). doi:10.1016/j.neuint.2010.12.004.

Zhou Y. *et al.*, Rapid separation and characterisation of triacylglycerols in ostrich oil by ultra performance liquid chromatography coupled with quadrupole time-of-flight mass spectrometry, *Food Chemistry*, 141 (3), 2098-2102 (2013). https://doi.org/10.1016/j.foodchem.2013.05.079